Advances in Water Resources 195 (2025) 104857

Contents lists available at ScienceDirect

Advances in Water Resources

journal homepage: www.elsevier.com/locate/advwatres

A Modeling framework for flocculated cohesive sediment transport in the current bottom boundary layer

Jorge A. Penaloza-Giraldo [a,b,*], Liangyi Yue [c], Tian-Jian Hsu [c], Bernhard Vowinckel [d], Andrew Manning [c,e,f], Eckart Meiburgc [g]

[a] Environmental Sciences Division and Climate Change Science Institute, Oak Ridge National Laboratory, Oak Ridge 37830, TN, USA
[b] Formerly at Department of Civil and Environmental Engineering, Center for Applied Coastal Research, University of Delaware, Newark 19716, DE, United States
[c] Department of Civil and Environmental Engineering, Center for Applied Coastal Research, University of Delaware, Newark 19716, DE, United States
[d] Institute of Urban and Industrial Water Management, Technische Universität Dresden, Dresden 01062, Germany
[e] HR Wallingford Ltd, Coasts and Oceans Group, Wallingford OX10 8BA, United Kingdom
[f] School of Biological and Marine Sciences, University of Plymouth, Plymouth PL4 8AA, Devon, United Kingdom
[g] Department of Mechanical Engineering, UC Santa Barbara, Santa Barbara 93106, CA, United States

ARTICLE INFO

Keywords:
Flocculation
Cohesive sediment transport
Population balance equation model
Current bottom boundary layer

ABSTRACT

Cohesive sediment transport, where its settling velocity is controlled by the flocculation process, is a crucial component in determining biochemical cycles, fate of pollutants, and morphodynamics in many aquatic ecosystems. In this study, a modeling framework is presented to investigate how flocculation influences cohesive sediment transport in the current bottom boundary layer in dilute conditions, consistent with the calibration range of the flocculation model. From a local analysis of floc dynamics in homogenous turbulence, we identify that the floc size distribution is mainly controlled by floc cohesion and yield strength. The uncertainty in fractal dimension plays a minor role for the floc size but it influences the resulting floc density and settling velocity. The transport analysis in the current boundary layer shows that the flocculation process alters the vertical distribution of the settling velocity and hence the sediment concentration with a strong dependence on cohesion, floc yield strength, and floc structure. When the flocs are more susceptible to breaking, a well-mixed concentration profile is obtained. In contrast, for flocs with higher cohesion or yield strength, higher concentration with a sharp gradient is observed close to the bed. Overall, the settling velocity exhibits a low vertical variability within 20 % of the depth-averaged value except near the bed. This suggests that using a depth-averaged settling velocity yields acceptable predictions of the sediment concentration profiles, especially for flocs with lower cohesion.

1. Introduction

Flocculation occurs when cohesive particles driven by environmental flows collide and stick together, generating aggregates, often called flocs, of different sizes. The resulting flocs are formed as a porous mixture of mineral and water that can encapsulate different substances (e.g., nutrients and organic matter), exerting a fundamental control on their fate via cohesive sediment transport (Amoudry and Souza, 2011; Winterwerp, 2002). For instance, cohesive sediment transport plays a critical role in shaping the morphology of estuaries and coastal areas (Edmonds and Slingerland, 2010; Friedrichs and Wright, 2004) and controls the dynamics of the estuarine turbidity maximum (ETM) (Burchard et al., 2018; Horemans et al., 2020). Flocculation impacts cycles of erosion and deposition of sediment and hence affects exchange rate of organic matters and gases with the seabed (Moriarty et al., 2018). Similarly, floc formations are part of freshwater fluvial system processes when biological effects are active (Lee et al., 2017; Osborn et al., 2023). Therefore, the study of flocculation and cohesive sediment transport are important research topics for ecological and engineering purposes.

Flocculation comprises two main processes denominated as aggregation and breakup (fragmentation). Although there are three fundamental mechanisms, namely, Brownian motion, differential settling, and turbulence that cause flocculation, turbulence is by far the most dominant mechanism in energetic environments. A commonly used parameter to quantify turbulence is the turbulent shear rate, which is responsible for generating a wide variety of flocs with different physical

* Corresponding author.
E-mail address: japg@udel.edu (J.A. Penaloza-Giraldo).

https://doi.org/10.1016/j.advwatres.2024.104857
Received 7 February 2024; Received in revised form 26 November 2024; Accepted 27 November 2024
Available online 28 November 2024

properties in size, shape, density, porosity, and settling velocity (Mietta et al., 2009; Spencer et al., 2022). Therefore, flocculation increases the complexity of cohesive sediment transport considerably (Wang et al., 2013). Through flocculation, the settling velocity becomes a variable in the modeling of the deposition flux, which affects the suspended sediment concentration in the water column (Sherwood et al., 2018). Accurate predictions for cohesive sediment transport demand the incorporation of flocculation models in modeling frameworks (Horemans et al., 2020; Sherwood et al., 2018; Winterwerp, 2002; Xu et al., 2010).

Flocculation models can be largely classified into three categories, the particle-scale approach (Vowinckel et al., 2019; Yu et al., 2022), the floc size distribution approach (Maerz and Wirtz, 2009), and the single floc size evolution approach (Winterwerp, 1998). The particle-scale approach tracks each individual cohesive particle, and it can simulate detailed flocculation dynamics in a fully-resolved turbulence field. Theoretically, this approach resolves flocculation dynamics and sediment transport in a holistic way. However, the challenge lies in its high computational cost, and existing simulations are mostly carried out in homogeneous turbulence that can hardly represent flow fields in practical aquatic systems (Zhao et al., 2021, 2023). Many modeling frameworks have been proposed to couple a cohesive sediment transport model with a flocculation model. Winterwerp (2002)developed a sediment transport model based on an advection-diffusion equation that also incorporates flocculation dynamics for median floc statistics. This model is the most computationally efficient, and a similar approach has been applied to study the effect of flocculation on the formation of ETM (Horemans et al., 2020). However, due to its simplification of the complex re-distribution of sediment mass among different size classes, it does not resolve the diversity of floc sizes and their properties. The compromising third approach either models the evolution of floc size distribution using their moments (Maerz and Wirtz, 2009) or directly resolves the Population Balance Equation (PBE) (Verney et al., 2011). This type of approach is more practical since floc properties (e.g., settling velocities and floc density) can be obtained with affordable computational cost and it (or its reduced form by Shen et al. (2018)) can be coupled with sediment transport models for Reynolds-averaged formulations (Sherwood et al., 2018; Xu et al., 2010) and 3D large-eddy simulations (Liu et al., 2019). Since the inhomogeneous flow field and the flocculation dynamics are modeled simultaneously, an affordable number of size classes used for the discretization of the floc size distribution is recommended to be around 15 for turbulence-averaged modeling in Sherwood et al. (2018) or 28 for 3D large-eddy simulation of Liu et al. (2019). These numbers are significantly lower than the recommended value of 75 by Penaloza-Giraldo et al. (2023), who carried out a comprehensive PBE model study for numerical convergence of floc size distribution and to match the measured coarse, medium and fine floc fractions obtained in the laboratory experiments of Keyvani and Strom (2014).

Flocculation has mainly been studied in saline coastal environments such as estuaries (Manning and Dyer, 2002; Wang et al., 2013), as salt is a controlling factor in floc formation (Krahl et al., 2022). However, image analysis of both in situ and laboratory data have revealed that floc composition in freshwater fluvial systems is similar to that found in estuaries (Fox et al., 2014; Lee et al., 2017; Spencer et al., 2022). This suggests that flocculation also occurs in the absence of salinity or in very low salinity (Krahl et al., 2022). A recent field study at the lowermost freshwater reaches of the Mississippi River confirms the existence of seasonal changes of concentration profiles due to the flocculation exacerbated by biofilms (Osborn et al., 2023). The need to investigate the effects of flocculation on cohesive sediment transport in fluvial and estuarine environments for a wide range of cohesion due to salinity variation and biological effects is warranted.

The primary goal of this study is to advance the understanding and modeling of how flocculation affects cohesive sediment transport processes in the bottom boundary layer. The specific objectives are to (1) develop a modeling framework that couples flocculation with cohesive sediment transport in the current bottom boundary layer, (2) evaluate how flocculation affects the floc size and settling velocity for a range of floc properties and environmental conditions, and (3) investigate how the variability of floc properties controls cohesive sediment transport in the current bottom boundary layer. The remainder of this paper is organized as follows. Section 2 presents a description of the modeling framework and data processing methods. Section 3 provides a local sensitivity analysis for the PBE flocculation model and main results from the modeling framework of cohesive sediment transport. Section 4 is dedicated to a discussion of the model applicability and limitations, and Section 5 concludes this study.

2. Model formulation

2.1. Model framework for dilute cohesive sediment transport

The model framework, driven by a turbulent shear rate profile S in a statistically-steady and fully-developed current bottom boundary layer, combines flocculation modeling to determine the floc settling velocity with sediment transport calculation in dilute conditions. The turbulent shear rate is defined as

$$S = \sqrt{\frac{\varepsilon}{\nu}} \tag{1}$$

where ε is the turbulence dissipation rate and ν is the fluid viscosity. The model framework consists of the following solution procedures, as illustrated in the flowchart shown in Fig. 1. The first step (Step I) is to provide a statistically (turbulence-) averaged shear rate S and sediment concentration Cprofiles in a current bottom boundary layer by assuming a constant settling velocity w_s. Here, we define the coordinate x_3 having its origin at the bottom and pointing vertically upward. These profiles are the input variables to the model framework, or they can be considered as the initial condition without considering flocculation dynamics. The PBE flocculation model is driven by these input profiles (Step II) to distribute sediment mass into different floc size classes at every vertical location (grid location) until each floc size class reaches the equilibrium state. The distributed floc properties from the flocculation model are used to calculate the weighted average settling velocity of the cohesive sediment W_a (see Step III in Fig. 1). This new settling velocity, which reflects the physics of flocculation, is used to update the sediment concentration profile in the boundary layer via an iterative procedure (Step IV). In a statistically-steady and fully-developed bottom boundary layer, sediment concentration $C(x_3)$ must follow the statistically averaged mass balance equation expressed as

$$K_s\frac{dC}{dx_3} + W_a C - \langle u_3' c' \rangle = 0 \tag{2}$$

where K_s is the sediment diffusivity, and the bracket "< >" is the turbulence-averaging operator. The turbulent flux of sediment $\langle u_3' c' \rangle$ requires a closure model and we adopt the gradient transport model written as

$$-\langle u_3' c' \rangle = K_t \frac{\partial C}{\partial x_3} \ . \tag{3}$$

where K_t is the turbulent diffusivity of the sediment. Substituting this approximation into the Eq. (2) leads to

$$\frac{dC}{dx_3} = -\frac{W_a C}{K_t + K_s}, \tag{4}$$

In a typical Reynolds-averaged models, K_t is estimated via the turbulent Schmidt number Sc_t and eddy viscosity ν_t as $K_t = \nu_t / Sc_t$. In this study, we obtain eddy viscosity, turbulent sediment flux, and turbulent shear rate S from direct numerical simulation (DNS) data (see Section

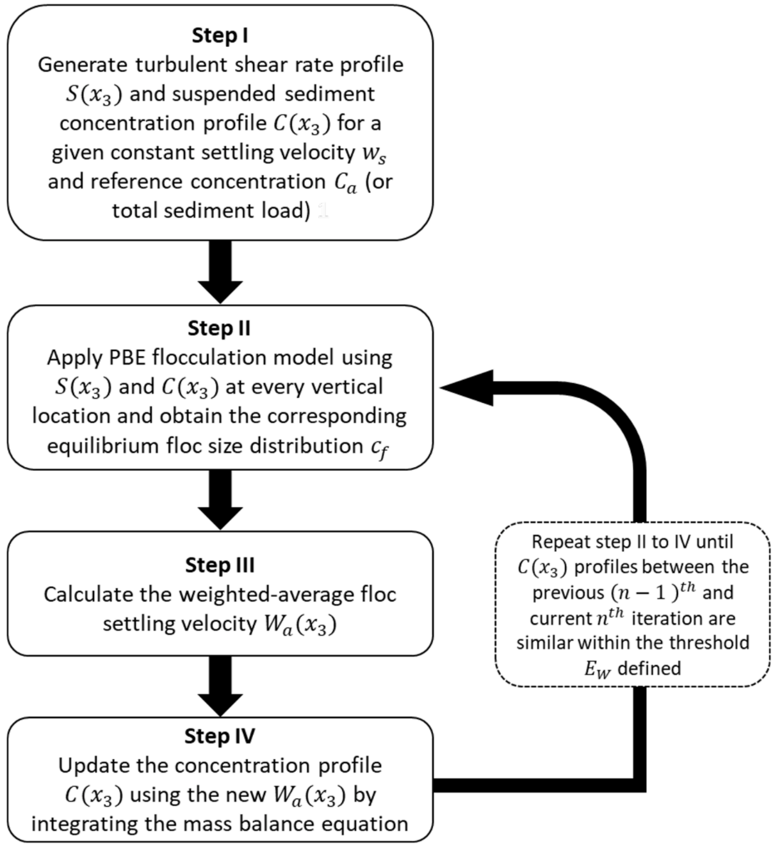

Fig. 1. A flowchart for the cohesive sediment modeling framework considering flocculation dynamics.

2.2), which resolves all turbulent scales, and K_t is directly calculated via Eq. (3) (see also Eq. (7)). More discussions on the K_t is presented in Section 4.

Eq. (4) is integrated numerically by forward finite differences to solve the vertical profile of averaged sediment concentration C provided that a bottom boundary condition is specified (see Step IV in Fig. 1). In this study, we enforce the total sediment mass throughout the water column to be conserved (the same as the initial total sediment mass) and a simple iteration is used, with a tolerance of $\varepsilon_C = 1 \times 10^{-6}\ kgm^{-3}$, to specify the bottom boundary value of $C_{x_3=0}$ via a gradual concentration increment $\Delta C|_{x_3=0} = 0.0001\ kg\ m^{-3}$. Finally, the new mass concentration profile $C^{(n)}$ and the pre-established turbulent shear rate S are used as inputs for the next iteration to obtain the flocculation properties and the weighted average settling velocity W_a. This iteration loop converges until the Root-Mean-Square difference E_w between the previously iterated settling velocity $W_a^{(n-1)}$ and the new $W_a^{(n)}$ is less than or equal to the tolerance $\varepsilon_W = 1 \times 10^{-6}$m/s. The key assumption in the present formulation is that the turbulent shear rate S is unchanged during the solution process. This assumption ignores the effect of sediment-induced density stratification on attenuating flow turbulence. However, this assumption is appropriate for the dilute flow considered in this study.

2.2. Direct numerical simulation data

DNS data is obtained by simulating a turbulent bottom boundary layer driven by a current assuming a constant sediment settling velocity (no flocculation) for dilute suspended sediment using the numerical model of Yue et al. (2020). Turbulence-averaged turbulent shear rate and sediment concentration profiles are used as inputs for the model framework (see Step I in Fig. 1). DNS for turbulent flow resolves all scales of turbulence and hence various turbulence statistics can be accurately calculated, such as the turbulent dissipation rate (see Eq. (1)).

Yue et al. (2020) calculated fine-grained sediment transport via an advection-diffusion equation in a computational domain defined as a rectangular prism with dimensions $L_1 \times L_2 \times L_3$, where the coordinate origin is located at the bottom left front corner, pointing in the streamwise x_1, spanwise x_2 and vertical x_3 directions (see Fig. 2). Periodic boundary conditions are implemented for the statistically-homogeneous streamwise (x_1) and spanwise (x_2) directions, while no-slip and free-slip boundary conditions are imposed at the bottom and top boundaries of the computational domain, respectively. The resulting current, driven by a prescribed streamwise pressure gradient, exerts a shear stress on the erodible cohesive sediment bed and suspends sediment into the computational domain if the bottom shear stress surpasses the critical shear stress, following the Partheniades-Ariathurai-type expression (Sanford and Maa, 2001). The sediment phase velocity is approximated by the flow velocity field plus a constant particle settling velocity of $w_s = 0.5mm/s$. More details of the numerical model formulation can be found in Yue et al. (2020).

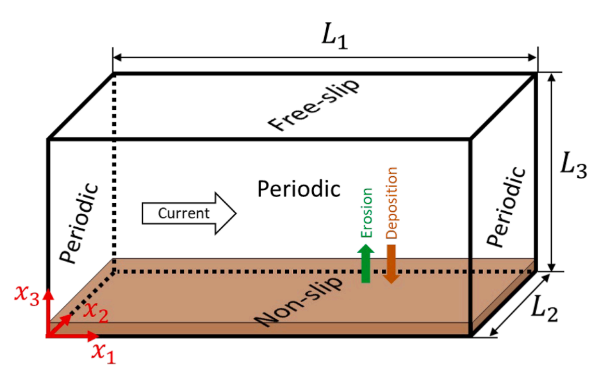

Fig. 2. Sketch of the computational domain including its boundary conditions.

Since the cohesive sediment modeling framework requires input of turbulence-averaged profiles (see Step I in Fig. 1), the streamwise velocity and sediment concentration fields from the DNS data are decomposed into statistically-averaged mean quantities, denoted by angular brackets $\langle \cdot \rangle_{12t}$. The subscript 1 and 2 indicates applying a plane average process in streamwise x_1 and spanwise x_2 direction while the subscript t corresponds to the time average after the flow reaches a statistical statistically-steady state. Hence, a turbulence-averaged quantity can be calculated by the following expression

$$\langle \psi \rangle_{12t}(x_3) = \frac{1}{T\,L_1 L_2} \sum_{t=t_0}^{t=t_0+T} \sum_{x_1=0}^{x_1=L_1} \sum_{x_2=0}^{x_2=L_2} \psi(x_1, x_2, x_3, t) \Delta x_1 \Delta x_2 \Delta t, \tag{5}$$

where ψ is a representative quantity, t_0 is the time instant at which the flow becomes statistically steady and T is the duration of time average. The turbulent fluctuation component $\psi'$is then obtained by the Reynolds decomposition

$$\psi'(x_1, x_2, x_3, t) = \psi(x_1, x_2, x_3, t) - \langle \psi \rangle_{12t}(x_3). \tag{6}$$

Using the fluctuating components of velocity u_i' and mass concentration c', the turbulent diffusivity of sediment K_t can be calculated from the DNS data as follows

$$K_t = -\frac{\langle u_3' c' \rangle_{12t}}{\frac{d\langle c \rangle_{12t}}{dx_3}}. \tag{7}$$

In this study, we use the DNS data as input to the modeling framework and Eq. (7) is applied directly to calculate the turbulent diffusivity. Similarly, the eddy viscosity can be calculated from the DNS data as

$$\nu_t = -\frac{\langle u_1' u_3' \rangle_{12t}}{\frac{d\langle u_1 \rangle_{12t}}{d_{x_3}}}. \tag{8}$$

The main driving force of flocculation is the turbulent shear rate S, or the turbulent dissipation rate ε (see Eq. (1)), which is determined by the environmental flow conditions. Here, the turbulent dissipation rate ε ($m^2 s^{-3}$) is calculated directly from the DNS data using its original definition as

$$\varepsilon = \nu \left\langle \left(\frac{\partial u_i'}{\partial x_j} \right)^2 \right\rangle_{12t} \tag{9}$$

The turbulent shear rate can be associated with the Kolmogorov length scale as $\eta = \sqrt{\nu/S}$, which means that the higher the turbulent shear S, the smaller the Kolmogorov length scale. Indeed, it is difficult to estimate the turbulent dissipation directly from measured data because it requires the calculation of spatial gradients of turbulent velocity fluctuations with a very high-resolution. A key reason for using DNS for the present study of flocculation and cohesive sediment transport is that it provides high resolution temporal and spatial data, allowing us to accurately calculate the turbulent dissipation rate. However, we must emphasize that for the general use of the modeling framework presented in Section 2.1, other estimations of the turbulent dissipation rate profiles via semi-empirical theory combined with measured data, or a two-equation Reynolds-average closure, are applicable as well.

2.3. Flocculation model and settling velocity

The open-source PBE flocculation model FLOCMOD (Verney et al., 2011) is utilized in the present modeling framework to compute the floc size distribution due to the flocculation processes (see Step II in Fig. 1). The PBEs describe the temporal evolution of the number concentration for each floc size class driven by a given local shear rate and sediment mass concentration, and they are written as

$$\frac{dn_f(k)}{dt} = G_{ag}(k) + G_{bs}(k) - L_{ag}(k) - L_{bs}(k), \tag{10}$$

where $n_f(k)$ (units in m^{-3}) is the number concentration for floc size class k. The terms G and L represent the gain and loss due to aggregation (subscript ag) and breakup processes (subscript bs) respectively. Since turbulent shear is the primary force driving flocculation in estuarine and coastal environments, other flocculation mechanisms such as Brownian motion and differential settling are neglected (Verney et al., 2011).

The gain G_{ag} and loss L_{ag} terms due to the aggregation can be defined as follows

$$G_{ag}(k) = \frac{1}{2} \sum_{i+j=k} \alpha A(i,j) n_i n_j, \tag{11}$$

$$L_{ag}(k) = \sum_{i=1}^{N_f} \alpha A(i,k) n_i n_k, \tag{12}$$

where N_f is the total number of floc size classes, and α is the collision efficiency, which parameterizes the sticking properties of the flocs. In this study, we assume that α is a constant following Verney et al. (2011). The floc collision is described by the collision probability function A for two colliding spherical particles driven by turbulent shear rate S, and it is written as

$$A(i,j) = \frac{1}{6} S \left(d_{f,i} + d_{f,j}\right)^3, \tag{13}$$

where d_f is the floc diameter for the i^{th} and j^{th} size class (McAnally and Mehta, 2000). The gain G_{bs} and loss L_{bs} due to turbulence are expressed as

$$G_{bs}(k) = \sum_{i=k+1} FDBS_{ki} B_i n_i \ , \tag{14}$$

$$L_{bs}(k) = B_k n_k, \tag{15}$$

where $FDBS_{ki}$ refers to the distribution function of fragmented flocs, representing the process by which daughter flocs in the k size class are generated from larger i floc size classes. Following Verney et al. (2011), we specify a binary distribution, meaning that each breakup event divides a floc into two equal halves. The function B describes the rate of breakage of the flocs break due to the turbulent shear rate S, and it is written as

$$B_i(k) = \beta S^{3/2} d_{f,i} \left(\frac{d_{f,i} - d_p}{d_p} \right)^{3-f_d}, \tag{16}$$

where d_p is the primary particle diameter, and f_d is the fractal dimension for equivalent spheres (Kranenburg, 1994). The fragmentation rate β is dimensional (unit $s^{1/2} m^{-1}$) and is defined as

$$\beta = E \left(\frac{\mu}{F_y} \right)^{1/2}, \tag{17}$$

where μ is the fluid dynamic viscosity, F_y is the floc yield strength and E is an empirical dimensionless parameter. In this study, we treat β as an empirical constant following previous studies (Maggi et al., 2007; Verney et al., 2011; Wang et al., 2013).

The fractal approach is adopted to model complex floc structures. The floc density ρ_f of the k^{th} floc size class is calculated by the corresponding floc diameter d_f as (Kranenburg, 1994)

$$\rho_f(k) = \rho_w + (\rho_p - \rho_w) \left(\frac{d_p}{d_f(k)} \right)^{3-f_d} \tag{18}$$

where ρ_p is the primary particle density and the fractal dimension is f_d. Following the same self-similarity concept, the sediment mass contained in each floc in size class k can be expressed as follows

$$m_f(k) = \rho_p \frac{\pi}{6} d_p^3 \left(\frac{d_f(k)}{d_p}\right)^{f_d}. \quad (19)$$

The floc settling velocity for each size class k is calculated by the Stokes' law using the corresponding flow density and diameter as

$$w_f(k) = \frac{(\rho_f(k) - \rho_w)\ g d_f^2(k)}{18\mu}. \quad (20)$$

By substituting Eq. (18) into Eq. (20), we obtain an explicit relationship between floc settling velocity and floc diameter for size class k as

$$w_f(k) = \frac{(\rho_p - \rho_w)\ g d_p^{3-f_d}}{18\mu}\ d_f^{f_d-1}(k). \quad (21)$$

The resulting distributed floc properties from the PBE flocculation model applied at each vertical location x_3 are used to calculate the weighted average quantities (see Step III in Fig. 1) as follows

$$\vartheta_a(x_3) = \sum_{k=1}^{N_f} \left(\frac{c_f(k)}{C(x_3)}\right) \vartheta_f(k), \quad (22)$$

where ϑ_f is an arbitrary distributed floc property (such as d_f, w_f or ρ_f) and ϑ_a is the corresponding weighted average quantity, $c_f(k)$ is the mass concentration in floc size k, which is defined as $c_f(k) = m_f(k) n_f(k)$.

3. Results

Cohesive sediment transport is generally a function of space and time. However, owing to the incorporation of the PBE flocculation model, the cohesive sediment variables further depend on the floc size distribution. The PBE flocculation model is designed to be driven by a given set of turbulent shear rate and sediment concentration in homogeneous turbulence conditions (Verney et al., 2011) and this is called local analysis in this study. In a typical cohesive sediment transport modeling framework (e.g., Sherwood et al. (2018) and including the present study), the PBE flocculation model is further applied at every local grid point and this is called a transport analysis. To better understand the PBE flocculation model and the resulting floc properties, a local sensitivity analysis is presented in Section 3.1, which is then followed by a transport analysis in Section 3.2. While an extensive local sensitivity analysis is reported by Verney et al. (2011), we present further local sensitivity analyses due to cohesive sediment properties and environmental forcing to enhance the understanding of cohesive sediment distribution and settling velocity variability in the transport analysis. A comprehensive sensitivity analysis of the PBE flocculation model for initial floc size distribution, number of size classes, primary particle properties and breakup types can be found in Verney et al. (2011).

3.1. Local analysis of the flocculation model

For a given set of cohesive particle parameters (i.e., collision efficiency α, fragmentarion rate β and fractal dimension f_d) and driving factors from the environmental flows (i.e., turbulent share rate S and the turbulence-averaged sediment concentration C), 246 simulations are performed (see Table 1). Following Penaloza-Giraldo et al. (2023), all simulations are discretized with $N_f = 75$ floc size classes distributed logarithmically for a better representation of the coarse floc fractions. The smallest floc size class in the modeled distribution corresponds to the primary particle diameter $d_p = 4\mu m$ and the maximum floc size is selected to be $\max(d_f) = 2500\mu m$. The floc size distribution is initialized by specifying the entire sediment mass at floc size class $d_f = 20\mu m$. Pure clay particles in the size range of 1~4 μm were rarely found in nature because once flocs are formed, flocs can rarely be broken back to the original clay particle for typical turbulence levels encountered. We used $d_f = 20\mu m$ as initial flocculi that typically exists in nature following Lee et al. (2012). As stated by Verney et al. (2011) and verified by Penaloza-Giraldo et al. (2023), the equilibrium floc size distribution is insensitive to the initial floc size distribution. Finally, the simulation time in each case is sufficiently long to ensure that all floc size classes reach the equilibrium state.

The collisional efficiency α, ranging from 0 to 1 according to Verney et al. (2011), quantifies the floc cohesion/stickiness in the aggregation process. A large value of α encourages floc growth. This direct proportionality can be noted when comparing the mass concentration distribution c_f at the equilibrium state for three different collisional efficiency values (see Scenario CSP1 in Fig. 3a). The lowest collisional efficiency value (i.e., α = 0.05) provides a mass concentration distribution c_f in the

Table 1
A summary of all cases simulated for local sensitivity analysis.

Local Sensitivity Analysis	Scenario	α	$\beta(s^{1/2}m^{-1})$	$r = \frac{\alpha}{\beta}$	$S(s^{-1})$	$C(kgm^{-3})$	f_d
Cohesive Sediment Parameters (CSP)	CSP1	0.05	0.02	2.5	50	0.1	2.0
		0.1	0.02	5.0	50	0.1	2.0
		0.2	0.02	10.0	50	0.1	2.0
	CSP2	0.1	0.04	2.5	50	0.1	2.0
		0.1	0.02	5.0	50	0.1	2.0
		0.1	0.01	10.0	50	0.1	2.0
	CSP3	0.1	0.02	5.0	50	0.1	2.0
		0.1	0.02	5.0	50	0.1	2.2
		0.1	0.02	5.0	50	0.1	2.4
Aquatic Environmental Variables (AEV)	AEV1	0.1	0.02	5.0	10	0.05	2.0
		0.1	0.02	5.0	50	0.05	2.0
		0.1	0.02	5.0	100	0.05	2.0
	AEV2	0.1	0.02	5.0	50	0.01	2.0
		0.1	0.02	5.0	50	0.05	2.0
		0.1	0.02	5.0	50	0.1	2.0
$\boldsymbol{W_a}$ affected by ratio $\boldsymbol{r}$ at different AEV	WCSP1	0.2	0.08	2.5	10~50	[0.01, 0.05, 0.1]	2.0
	WCSP2	0.2	0.02	10.0	10~50	[0.01, 0.05, 0.1]	2.0
$\boldsymbol{W_a}$ affected by ratio $\boldsymbol{f_d}$ at different AEV	WFD1	0.05	0.02	2.5	10	[0.01, 0.05, 0.1]	2.0
		0.05	0.02	2.5	10	[0.01, 0.05, 0.1]	2.2
		0.05	0.02	2.5	10	[0.01, 0.05, 0.1]	2.4
	WFD2	0.05	0.02	2.5	40	[0.01, 0.05, 0.1]	2.0
		0.05	0.02	2.5	40	[0.01, 0.05, 0.1]	2.2
		0.05	0.02	2.5	40	[0.01, 0.05, 0.1]	2.4
$\boldsymbol{t_e}$ with constant $\boldsymbol{r}$ at different AEV	ETF1	0.2	0.08	2.5	10~50	[0.01, 0.05, 0.1]	2.0
	ETF2	0.05	0.02	2.5	10~50	[0.01, 0.05, 0.1]	2.0